Pramana – J. Phys., Vol. 37, No. 4, October 1991, pp. 373–385. © Printed in India.

An automated laboratory EXAFS spectrometer of Johansson type: indigenous development and testing

S K DESHPANDE, S M CHAUDHARI, ASHOK PIMPALE*, A S NIGAVEKAR, S B OGALE and V G BHIDE

Department of Physics, University of Poona, Pune 411 007, India
*Present Address: IUC–DAEF, University Campus, Khandwa Road, Indore 452 001, India

MS received 8 July 1991

Abstract. An automated linear laboratory EXAFS spectrometer of the Johansson type has been indigenously developed. Only two translational motions are required to achieve the necessary Rowland circle configuration for the (fixed) X-ray source, the dispersing and focusing bent crystal and the receiving slit. With the available crystals the spectral region from 5 to 25 keV can be scanned. The linear motions of the crystal and receiving slit including the detector assembly are achieved by employing software-controlled DC motors and utilizing optical encoders for position sensing. The appropriate rotation of the crystal is achieved by the geometry of the instrument. There is a facility to place the sample alternately in the path of the X-ray beam and out of the path to record both the incident X-ray intensity I_0 and the transmitted intensity I employing the scintillation detector. An arrangement with a two-window proportional detector before the sample to measure I_0 and the scintillation detector to record I is also developed; in this case it is not necessary to oscillate the sample. Fast electronic circuits are employed to minimize counting errors. The instrument is user-friendly and it is operated through a menu-driven IBM compatible PC. EXAFS spectra of high resolution have been recorded using the spectrometer and employing the Si(111) reflecting planes; the X-ray source being a Rigaku 12 kW rotating anode with Cu target. We describe the spectrometer and discuss its performance with a few representative spectra.

Keywords. EXAFS spectrometer; Johansson type.

PACS Nos 07·85; 82·80

1. Introduction

The undulations in the absorption coefficient as a function of X-ray energy on the high energy side of an absorption discontinuity, extending sometimes to more than a thousand eV, have been known for a long time. Historically, these oscillations have been termed variously as Kossel structure in atoms and molecules and Kronig structure in the condensed phase. It took a very long time to understand the physical origin of this fine structure and even to-date the problem has not been completely understood. The earlier attempts at understanding this phenomenon were focused on interpreting these oscillations in terms of either the short range order or the long range order seen by the photoelectron (Azaroff 1963). The first breakthrough came when Lytle introduced a simple potential model based on a short range order theory (Lytle 1966). This model was generalized by Mande and co-workers (Deshmukh *et al* 1976) who attempted to give some physical interpretation of Lytle's potential. Lytle and co-workers realized that the fine structure can be split into two parts – the near

edge structure or XANES and the extended fine structure or EXAFS. After a lot of numerical work and analysis of a large amount of experimental data they showed that the fine structure can be used to obtain quantitative structural information (Sayers *et al* 1971). Stern later provided a general theory of EXAFS and showed that the scattering of the photoelectron from neighbouring atoms was the dominant mechanism responsible for EXAFS (Stern 1974). Subsequently, various methods of data analysis to obtain physical information were put forward (Lytle *et al* 1975; Stern *et al* 1975). It was thus clear that EXAFS can yield important structural information in a wide variety of materials. EXAFS can be used to study crystalline and amorphous solids, supported catalysts, biological materials, liquids and even polyatomic gases.

The early experiments on EXAFS were carried out on spectrometers with Cauchois type bent crystals and photographic plates. The low flux of X-ray from conventional X-ray sources limited the speed with which a spectrum could be recorded, and the experimental verification of some theoretical aspects was also not immediate. The situation improved a little when photon detectors and the associated electronic circuits were developed. The most significant improvement was provided by the development of synchrotron X-ray sources. The large X-ray flux over a wide energy range that was available from synchrotron sources made it possible to record high resolution spectra of a variety of materials in a very short time. There was considerable improvement in the quality of experimental data. However, it was not possible for most workers to use synchrotron sources because of their inaccessibility. The time available to each worker at a synchrotron beam line is limited which means there is not much opportunity for experimentation and immediate implementation of new ideas. A laboratory EXAFS facility which would give data of quality comparable to that obtainable at synchrotron facilities would be most useful. The development of rotating anode X-ray sources made this possible and several laboratory EXAFS spectrometers which could give spectra of high resolution comparable to the spectra obtained at synchrotron facilities have been developed in various laboratories. Apart from providing more time for experimentation, experiments requiring modification in apparatus, like temperature-dependent studies and other in situ experiments are possible with an in-house laboratory facility. An experiment can also be performed several times to optimize the sample characteristics.

In the Indian context, although much work has been done in the field of X-ray spectroscopy in general and EXAFS in particular, there is a lack of dedicated EXAFS spectrometers. In fact, an automated indigenous EXAFS facility utilizing a rotating anode and fast counting systems is almost non-existent. In addition, synchrotron radiation facilities are also not available, though INDUS 1 and 2 are expected to be ready in a few years time. It was felt that a laboratory spectrometer which is capable of recording spectra of high quality was necessary.

With this aim the present work of indigenous development of such a laboratory EXAFS spectrometer was undertaken. Our spectrometer is based on the design of Tohji *et al* (1983). It is completely automated and is capable of providing high resolution spectra in short scan times. The design of the spectrometer is given in § 2. Section 3 deals with the mechanical construction and § 4 describes the X-ray source and monochromator crystals. In § 5 we describe the control and data acquisition, in § 6 the alignment and in § 7 the performance, with a few representative spectra.

2. Design selection

Several laboratory EXAFS spectrometers have been developed with the aim of obtaining high resolution spectra in short scan times and minimum manual intervention (Koningsberger 1988). Almost all utilize the Rowland circle focusing geometry with bent crystal monochromators of either the Johann or Johansson type. Different mechanisms have been developed to hold the Rowland configuration while scanning. Some spectrometers use conventional sealed X-ray tubes as sources and the X-ray source is moved along with other components during a wavelength scan. Most use a rotating anode X-ray source which is fixed and thus one has to rotate as well as linearly translate the monochromator crystal and sample-detector stage. These are the so-called linear spectrometers. The positioning of the monochromator and the receiving slit of the sample-detector stage for three different angular settings, corresponding to three different wavelengths, is shown in figure 1 for the case of a linear spectrometer with a fixed source. The centre of the Rowland circle moves along a circle whose centre lies at the source position. The various spectrometers differ mainly in the way the crystal and other components are rotated and linearly translated while holding the Rowland circle configuration.

Note that the line joining the crystal centre C_1 and the centre of the Rowland circle O_1, when extended to C′ so that $C_1C_1' = 2R$ (R being the radius of the Rowland circle) the angle subtended by C_1C_1' at the anode is always $\pi/2$. Since the direction AC_1 is the fixed

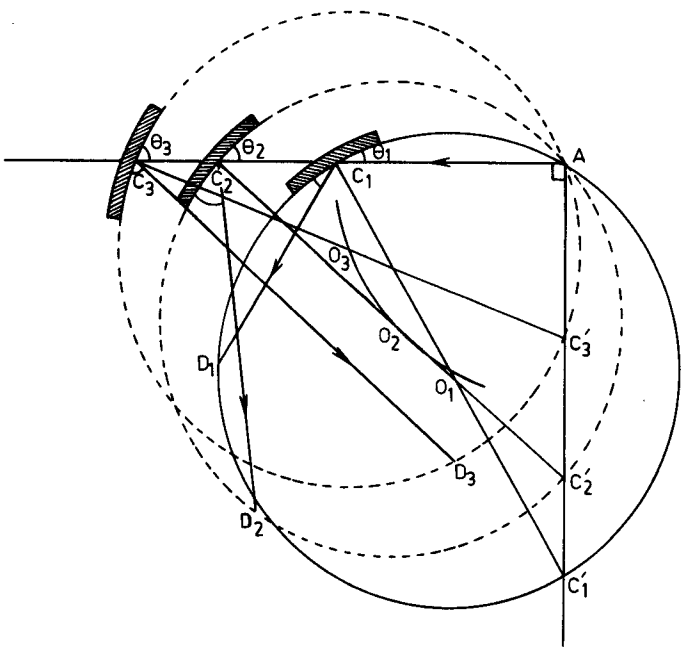

Figure 1. Geometry of a linear spectrometer with a fixed X-ray source A. C_1, C_2 and C_3 are the positions of centre of the monochromator for three different Bragg angles θ_1, θ_2 and θ_3, respectively. O_1, O_2 and O_3 are the corresponding positions of the centre of the Rowland circle.

incident direction of the X-rays, the locus of C_1' for different Bragg angles is thus along a direction at right angle to the incident direction. This is one of the main points utilized in the mechanical design of our spectrometer. The design is essentially simple requiring only two linear translations to scan any energy region of interest. There are few independently moving parts, which makes the instrument easy to control using a computer and also avoids errors in positioning. It is also convenient for changing monochromators and samples, and using different types of detectors. Different types of sample cells can also be used with ease. The number of joints in the mechanical components is not large. The assembly of the spectrometer and its alignment can be carried out easily. The use of Johansson crystals allows large intensity from the source to be focused on the sample. The Rowland circle radius can be changed to suit available crystals by only a few modifications. The spectrometer can be constructed using indigenous materials.

The geometry of the spectrometer is shown in figure 2. The anode A of the X-ray generator, the centre of the monochromating crystal C and the receiving slit R_1 are held on a Rowland circle of radius R by two bars and leads L_1 and L_2. L_1 and L_2 are perpendicular to each other and their point of intersection lies exactly below the anode focus A. The crystal C is held at one end of a bar of length $2R$ such that the crystal normal is parallel to the bar. One end of the bar translates along L_1 and the other end slides freely along L_2. The motion along L_1 is generated by a motor M_1.

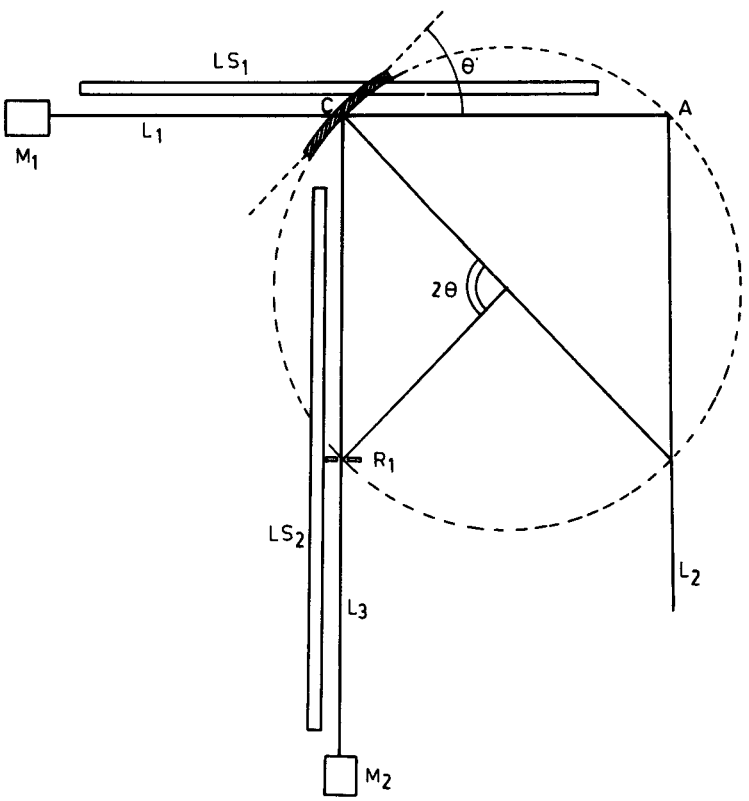

Figure 2. Schematic diagram of the linear EXAFS spectrometer. A: rotating anode focal spot; C: centre of monochromator crystal; M_1, M_2: DC motors; L_1, L_3: lead screws; L_2: linear bearing; LS_1, LS_2: linear optical encoders; R_1: receiving slit.

In this way, the translation along L_1 changes the glancing angle θ at the crystal C. The receiving slit, sample and detector are placed on a lead L_3. A bar of length R, connecting the receiving slit and the centre of the bar of length $2R$, determines the direction of L_3. In order to maintain the receiving slit on the Rowland circle a motor M_2 is used, driving the slit along L_3 such that the distance r_1 between anode and crystal is always equal to the distance r_2 between crystal and receiving slit. Thus, the angle between the two bars is always 2θ. L_3 moves freely in the horizontal plane. It is thus clear that only two translations are required to scan any wavelength region.

We have introduced the following modifications to the original design:

(a) The radius of the Rowland circle has been increased to 400 mm to obtain higher resolution. Also, crystals of large radius have relatively less imperfections and give a better performance.

(b) Linear optical encoders have been used to determine position along L_1 and L_3. These positions are fed to a computer program which controls the motor movement. The optical scales have a linear resolution of 5 μm.

(c) Motors M_1 and M_2 are DC synchronous motors. These provide better acceleration and the positioning can be more accurate.

(d) A scintillation detector has been used instead of a solid-state semiconductor detector as it is cheaper.

(e) We have used ordinary ball bearing for convenience in achieving smooth movement of L_3 along the horizontal plane.

A detector stage for two detectors, with the sample holder between the two detectors, has also been made for simultaneous measurement of the incident (I_0) and transmitted (I) X-ray intensity. A two-window proportional detector is then employed to measure I_0.

From figure 1, we see that

$$r_1 = r_2 = r = 2R\sin\theta = n\lambda R/d \tag{1}$$

where r_1 and r_2 are the distances between anode and crystal and crystal and receiving slit respectively, R is the Rowland circle radius, λ is the wavelength of X-rays, d is the interplanar spacing of the crystal reflecting planes and n is the order of diffraction.

3. Mechanical construction

The mechanical fabrication was carried out using indigenous components. A linear bearing was used as L_2 (see figure 2). Lead screws L_1 and L_3 were mounted along channels with slides to move the respective components along them. A straight bar with a V-shaped end was mounted along L_2 to hold the anode focal spot. The entire assembly was mounted on a plate on freely rotating balls so that the assembly can be rotated about the vertical axis passing through the focal spot. This allows alignment with respect to the take-off angle of X-rays. This plate is mounted on a base plate equipped with three screws for levelling the spectrometer. The end of mechanical motion is signalled by microswitches mounted at each end of L_1 and L_3. Due to mechanical constraints, the angular range that can be scanned is 10° to 70°. This corresponds to a minimum distance of crystal to source of about 139 mm and a maximum distance of about 752 mm. A crystal holder capable of rotating the crystal

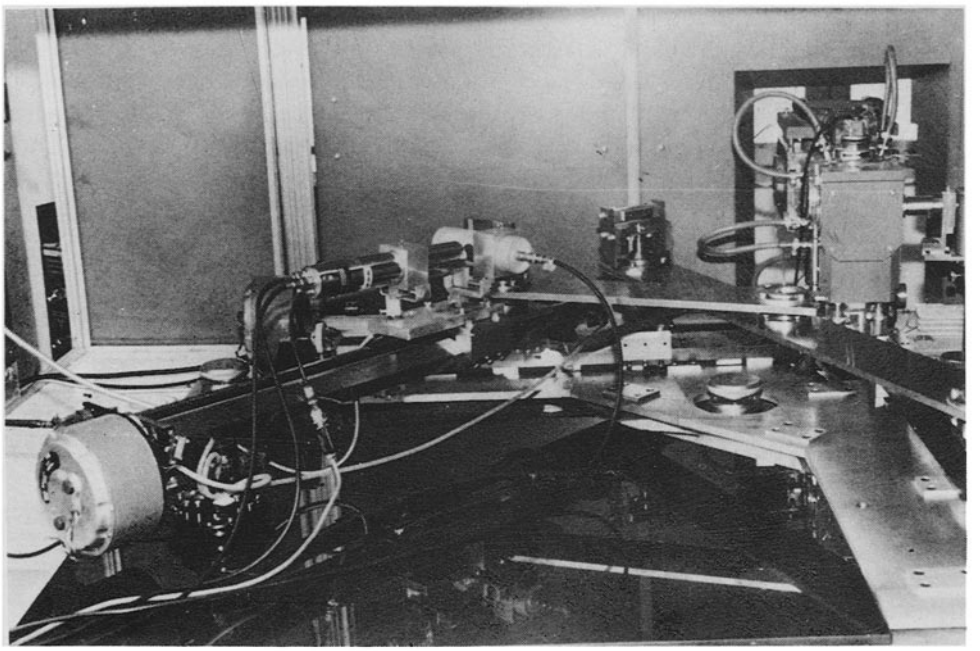

Figure 3. Photograph of the complete spectrometer after assembly.

about the horizontal and vertical axes, and moving it vertically, was made and mounted at the position C. A stepper motor has been used to oscillate the sample in and out of the beam path when this type of measurement is desired. Another assembly to hold two detectors and sample between them has also been made. Precision ball bearings were used at all joints where free rotation is required. The movement of the mechanical parts was checked using a dial gauge with an accuracy of 10 μm. The smooth movement of L_3 along the horizontal plane was achieved by using freely rotating balls under the supporting assembly for M_2. A photograph of the complete spectrometer is shown in figure 3.

4. X-ray source and monochromator crystals

We have used a 12 kW rotating anode X-ray generator (Rigaku RU-200, 60 kV, 200 mA) with a focus size of 0·5 mm × 10 mm. This can provide the high flux necessary for good quality EXAFS spectra. Although different anode materials can be used, we have used a copper anode. The take-off angle is 6°.

Johansson-type ground and bent crystals of different materials were obtained from Quartz et Silice, France. The size of the crystals is 15 mm × 50 mm and radius of Rowland circle is 400 mm. The larger dimension in the horizontal plane makes it possible to collect almost all the radiation from the source. Crystals with different interplanar spacings make it possible to scan different X-ray energy regions within the constraints of the available angular range. Table 1 shows the ranges that can be scanned in the first order by each of the crystals available in our laboratory.

Table 1. Energy ranges that can be scanned by different monochromator crystals within the constraints on the glancing angle θ*.

Crystal	Reflection	d (Å)	Energy at $\theta = 70°$ E_{min}(eV)	Energy at $\theta = 10°$ E_{max}(eV)
Ge	111	3·260	2023	10950
Si	111	3·135	2104	11388
Ge	311	1·703	3875	20968
Si	311	1·633	4040	21862
LiF	220	1·424	4633	25070

* The useful energy range of X-rays available from the source presently used is about 5 keV to 25 keV. The table indicates the energy range that is possible considering the crystals alone.

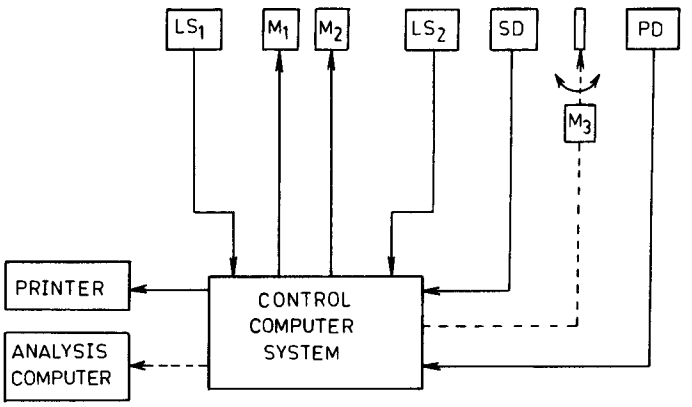

Figure 4. Schematic of the control and data acquisition system.

5. Control and data acquisition

In order to handle the high flux from a rotating anode X-ray source, a fast detection system must be used. We have used a scintillation detector (Canberra 1702) supported by fast electronic circuits to minimize counting loss. The control and detection system is shown schematically in figure 4. A microcomputer (IBM–PC) is used to control the motion of motors M_1 and M_2. The position of the crystal and receiving slit is determined using eq. (1) and the movement of motors M_1 and M_2 is controlled accordingly, with a preset point as reference. The position of the crystal along L_1 and that of the receiving slit along L_3 is constantly read by the linear optical scales LS_1 and LS_2, respectively. This position is fed back to the computer which ensures accurate positioning of both the crystal and the receiving slit. The speed of motion of the motors is varied as a function of distance of the current position from the required position, so that as the required position is approached, the motors slow down. Thus, any overshoot is eliminated and the positioning accuracy is maintained. A third motor M_3 may be used if sample oscillation is desired, in which case only the scintillation detector with a Canberra 2020 amplifier is used. In this mode, which we shall call mode A, the motor M_3 alternatively moves the sample in front of the

receiving slit when the transmitted beam intensity is measured, and out of the beam path when incident intensity is measured. In the second mode, which we shall call mode B, the sample is placed between a two-window gas filled proportional detector and the scintillation detector. The incident intensity (I_0) is measured by the proportional detector and the transmitted intensity (I) is measured by the scintillation detector simultaneously. The output of the scintillation and proportional detectors is given to the counting circuit after amplification. The counting circuit consists of two single channel analysers, one for each detector.

A convenient menu-driven computer software has been developed for control and data acquisition. The limiting values of the angle 2θ or the limiting values of energy of X-rays in the region to be scanned, the increment in angle or energy, and the time for counting at each position are the only initial parameters to be given to the computer for recording a spectrum. The incident intensity (I_0), the transmitted intensity (I) or the ratio of the two (I_0/I), can be plotted on screen during scanning. This makes it possible to view the spectrum while it is being recorded. The parameters like limiting values of energy or angle in a region, the step in angle or energy, the time per reading, the values of I and I_0, the ratio (I_0/I) and the current position of the crystal and sample, are all displayed on the computer monitor screen. The region of interest can be divided in as many as five sub-regions, each with a different increment in energy or angle θ. This allows recording data with a small increment only where required and a larger increment may be given in other regions, thereby reducing time for recording a spectrum. Data can be directly printed on a dot-matrix printer connected to the computer and provision has been made for copying the acquired spectrum on a floppy diskette. A stored spectrum can also be loaded from a floppy diskette on to the screen. Another computer for data analysis may be connected to the control computer.

6. Alignment of the instrument

The spectrometer has to be aligned with respect to the take-off angle of X-rays from the anode, the height of the beam above the base plate, and the location of the focal spot on the anode. The anode focal spot has been projected below the rotating anode assembly by a vertical pin. The intersection point of L_1 and L_2 must lie exactly below the focus (see figure 2). This can be achieved by making use of the bar along L_2 which has a V-shaped end. The vertical pin below the anode is held in the V-shaped end of the bar, ensuring that the anode focal spot lies exactly at the point of intersection as required. The plate on which the spectrometer is mounted was rotated about a vertical axis through this point. The position of the plate was fixed after ensuring that the X-ray beam falls on the crystal for different positions of the crystal along L_1. The X-ray beam was observed using a fluorescent screen. Levelling of the base plate was done with the three screws provided. This completes the alignment with respect to take-off angle and height of the X-ray beam. The crystal height and orientation were adjusted by moving the crystal holder vertically and rotating it about a horizontal axis, and using a fluorescent screen to observe the monochromatised beam. The characteristic emission lines $K\alpha_1$ and $K\alpha_2$ of copper source were used for calibration. The initial position of the crystal and receiving slit is determined by the first marker on corresponding linear encoder. This position was determined to an accuracy of 5 μm by using the $CuK\alpha_1$ and $K\alpha_2$ lines. The distances r_1 and r_2 are measured with reference to this initial position.

7. Performance

In this spectrometer two modes of measurement, modes A and B are possible, as mentioned above. The second mode requires less time for recording a spectrum than the first mode, and data is free from source fluctuations. We have observed the characteristic emission lines CuKα_1 and CuKα_2 of copper anode, using Si(111) crystal and the scintillation detector. Figure 5 shows this spectrum. This was recorded with a detector voltage of 740 V. It was observed that both the shape of the lines and their intensity ratio are very sensitive to the detector voltage, and the best spectrum obtained is shown here. The ratio of the intensities of the Kα_1 line to that of the Kα_2 line is about 2:1. After fitting a Lorentzian peak shape to each of these lines, we measured the FWHM of the CuKα_1 line as 9·7 eV. The CuKβ_1 line was also observed and its intensity was about one-fifth the Kα_1 intensity. This spectrum is not shown here for the sake of brevity. It may be mentioned that the detector and amplifier settings need not be the same and may have to be varied to record a good EXAFS spectrum.

An EXAFS spectrum of copper metal foil at room temperature recorded in mode A is shown in figure 6. This was recorded in 90 min using Si(111) monochromator and scintillation detector. The receiving slit width was 50 μm and the X-ray generator voltage and current were 14 kV and 50 mA, respectively. The fine structure is seen very clearly. This spectrum is comparable to that obtained by others (Tohji *et al* 1983; Cook and Sayers 1981). The EXAFS spectrum reported by Cook and Sayers 1981 is shown for comparison in figure 7. The EXAFS function obtained after pre-edge background removal and normalization of the fine structure, is shown in figure 8. The Fourier transform of this EXAFS function over the range of 3 Å^{-1} to 12 Å^{-1} in the

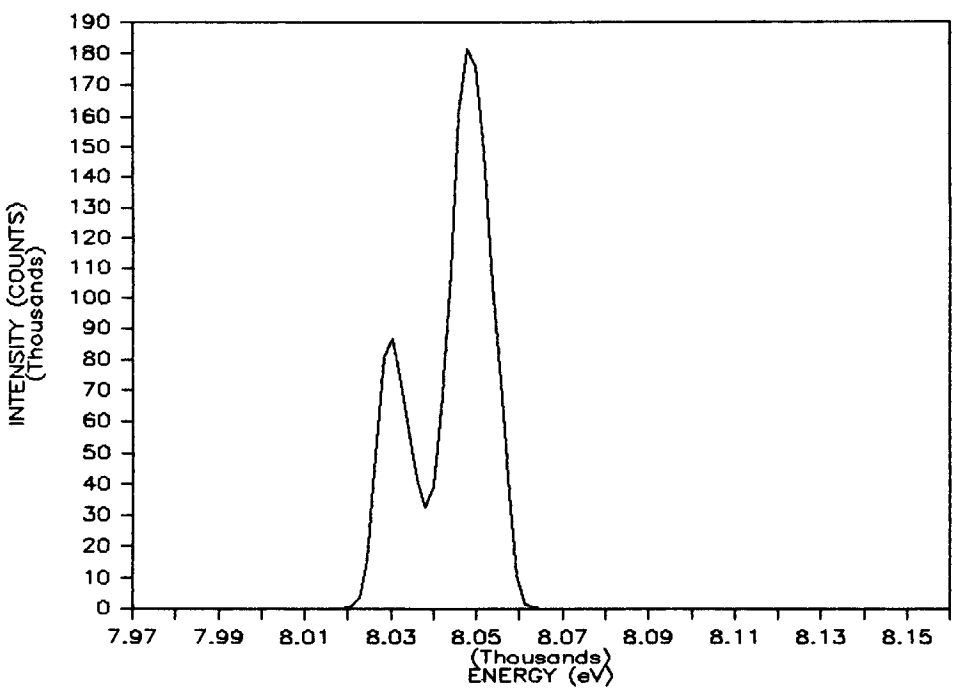

Figure 5. Kα_1 and Kα_2 emission lines of copper source recorded with Si(111) monochromator crystal.

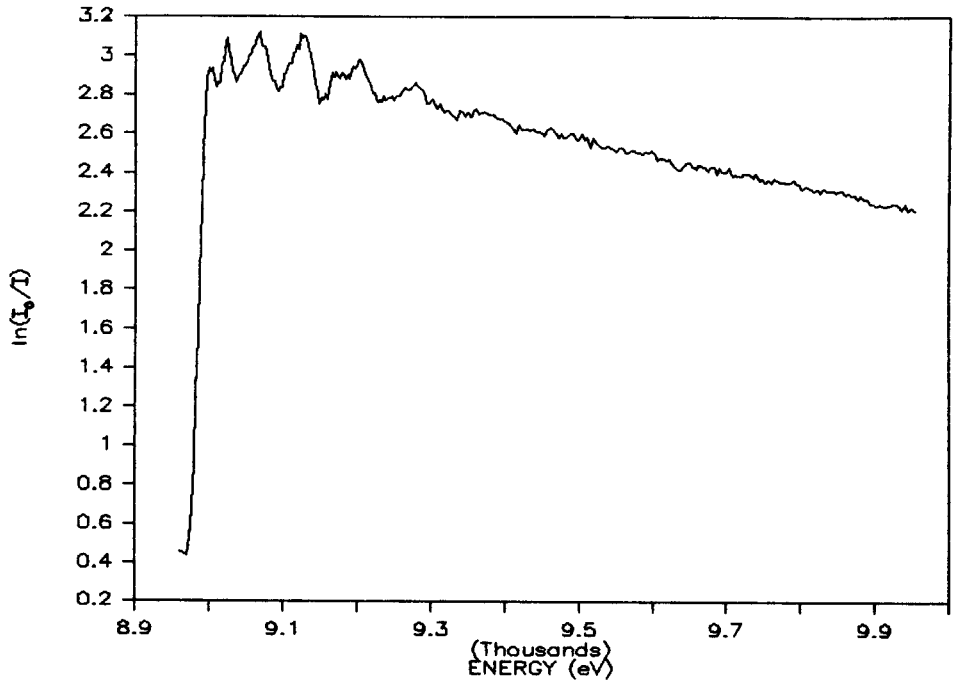

Figure 6. Copper foil EXAFS spectrum recorded with Si(111) monochromator in 90 min.

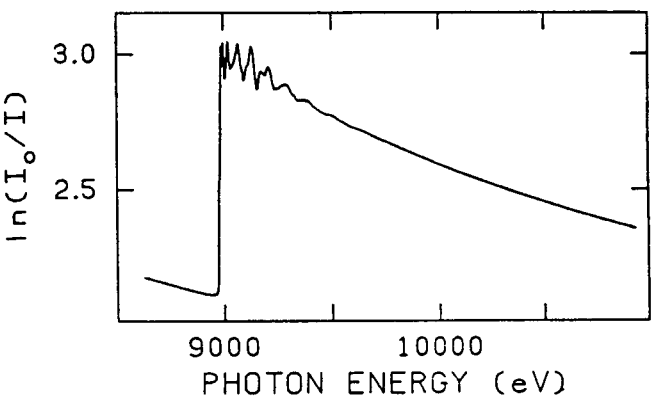

Figure 7. The EXAFS spectrum for copper foil reported in Cook and Sayers (1981).

photoelectron wave vector k is shown in figure 9 which can be compared with the radial distribution function.

We have used a self-contained Fortran program package developed by Indrea and Aldea (Indrea and Aldea 1980) for computation of the normalized EXAFS function and its Fourier transform. This program has been suitably modified for our requirements. The values of I_0 and I, the initial value of θ and the increment in θ are used as input parameters to compute the absorption coefficient using the relation

$$\mu x = \ln(I_0/I).$$

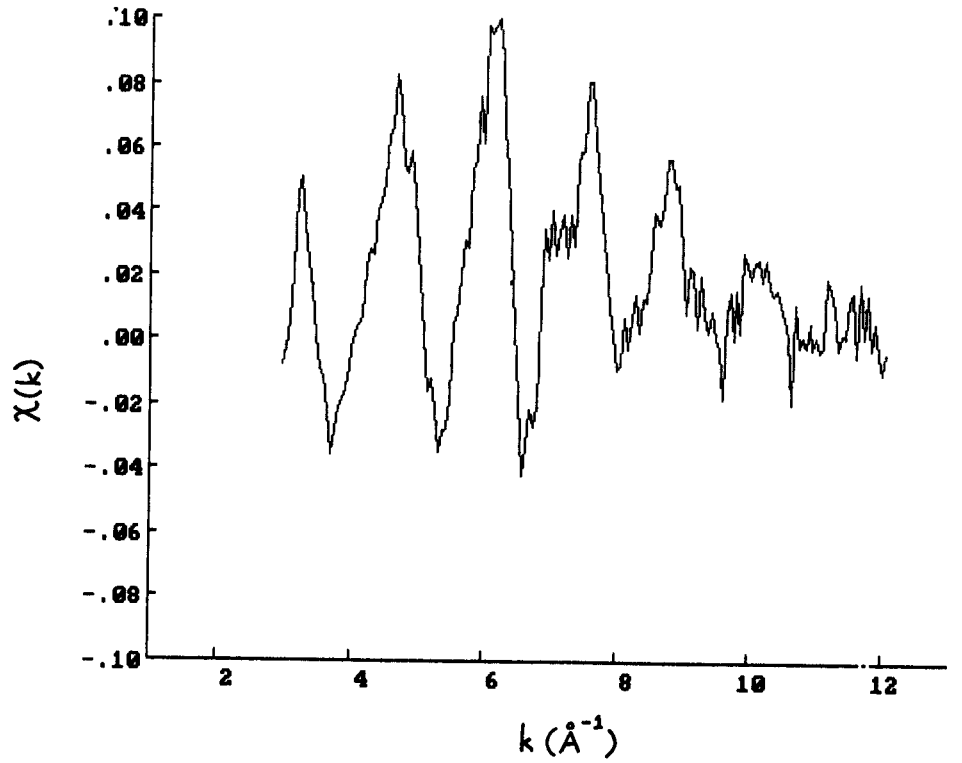

Figure 8. EXAFS function obtained from the spectrum of figure 6.

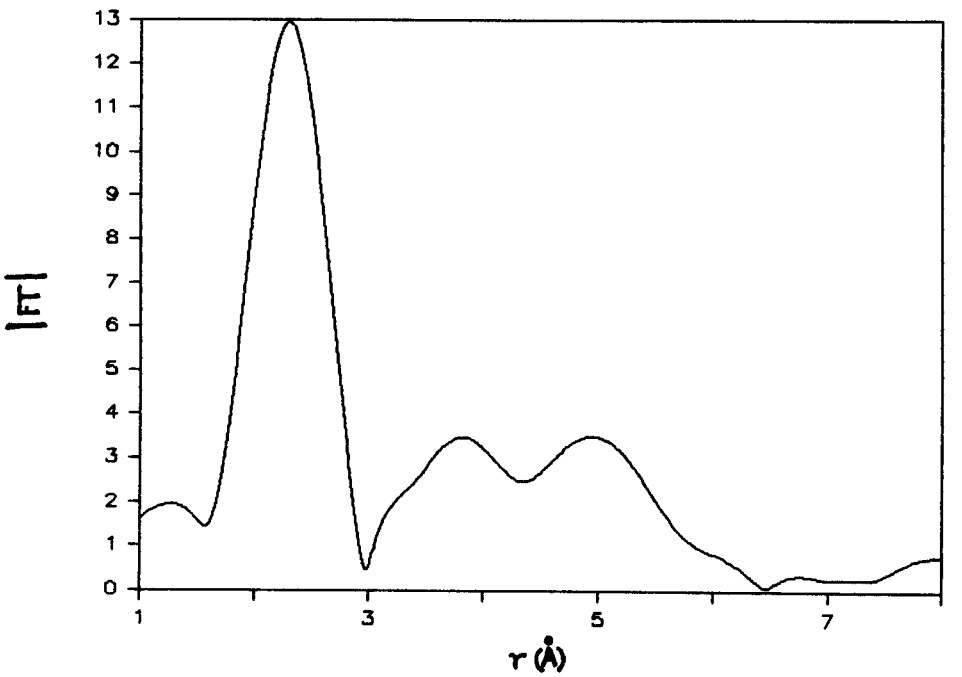

Figure 9. The Fourier transform of the EXAFS function shown in figure 8. The phase shift has not been taken into account.

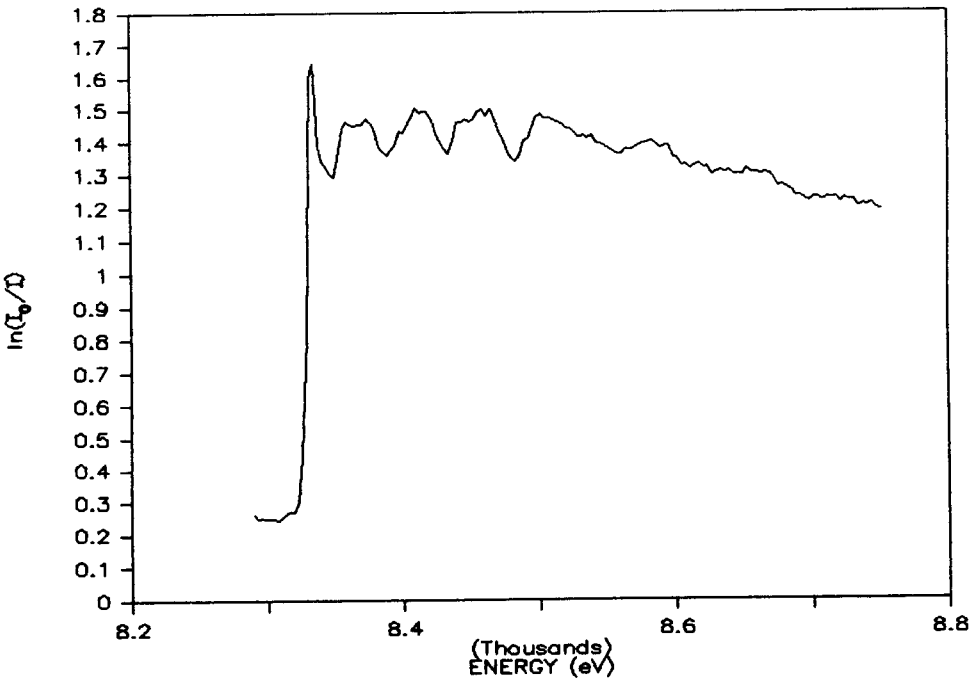

Figure 10. EXAFS spectrum of nickel powder recorded with Si(111) monochromator.

The program can perform background subtraction by fitting a Victoreen function of the form $A\lambda^4 + B\lambda^3$ to the pre-edge data and extrapolating this into the EXAFS region. A smooth function is used as an approximation for μ_0 and the normalized EXAFS function is computed according to the formula

$$\chi(k) = (\mu(k) - \mu_0(k))/\mu_0(k).$$

The Fourier transform of $k^n\chi(k)$ has been computed using Filon's quadrature formula (Abramowitz and Stegun 1965). The value of n can be varied (typically, $n = 0$, 1, 2 or 3) and the range in k which is used in the Fourier transform can be selected. A Hanning window function has been used to minimize truncation ripples due to finite data range. The corrections for phase shift have not been made. Further analysis like inverse Fourier transform of the first shell peak in the radial distribution function and the determination of structural parameters by iterative least squares fitting can also be carried out by using this program. The total running time for obtaining the spectra shown here was less than 3 min on an IBM PC–AT.

It is clear from figures 6–9 that spectra of good quality suitable for EXAFS studies can be obtained using this spectrometer. Another spectrum of Ni powder at room temperature, recorded in the same mode using Si(111), is shown in figure 10.

8. Conclusion

We have described an automated laboratory EXAFS spectrometer that has been fabricated indigenously, the only imported parts being the focusing crystals and the detection systems. We have also reproduced some representative spectra recorded on

this spectrometer. Although two modes of measurement are possible, mode A is not convenient in cases where absorption is large and one has to use an intense beam of X-ray, as counting errors may be introduced due to the saturation of the detection system. In such cases the second mode, mode B with two detectors may be used. This mode also reduces the time required for recording a spectrum. Another advantage of this mode is that temperature-dependent studies, or studies on liquid samples etc., may be carried out. This is not possible when the sample has to be oscillated, as is the case in the first mode. Accurate positioning of spectrometer components has been achieved by the use of linear optical encoders with a computer program for position sensing and control. Use of DC synchronous motors M_1 and M_2 provides better acceleration and improves performance of the spectrometer. We may mention here that the spectrometer can also be used for XANES studies. A menu-driven control and data-acquisition program makes the spectrometer easy to operate. The spectrometer is thus a convenient facility for high resolution EXAFS studies.

Presently, measurements are being carried out on several types of materials, particularly copper K-edge in doped high temperature superconductors and copper, nickel and iron edges in some metallic glasses. The results shall be described separately in other publications. Work is also in progress to develop an ab initio EXAFS program taking into account the lack of spherical symmetry and multiple reflections of the ejected photoelectron.

Acknowledgements

This work was supported by a research grant from the DST, New Delhi. One of the authors (SKD) would like to thank CSIR, New Delhi for a Junior Research Fellowship.

References

Azaroff L V 1963 *Rev. Mod. Phys.* **35** 1012
Abramowitz M and Stegun I A 1965 *Handbook of mathematical functions* (New York: Dover) p. 890
Cook J W and Sayers D E 1981 *J. Appl. Phys.* **52** 5024
Deshmukh P, Deshmukh P and Mande C 1976 *Pramana – J. Phys.* **6** 305
Indrea E and Aldea N 1980 *Comput. Phys. Commun.* **21** 91
Koningsberger D C 1988 *Laboratory EXAFS facilities* in *X-ray absorption*, (eds) D C Koningsberger and R Prins (New York: John Wiley) p. 163
Lytle F W 1966 *Adv. X-ray Anal.* **9** 398
Lytle F W, Sayers D E and Stern E A 1975 *Phys. Rev.* **B11** 4825
Sayers D E, Stern E A and Lytle F W 1971 *Phys. Rev. Lett.* **27** 1204
Stern E A 1974 *Phys. Rev.* **B10** 3027
Stern E A, Sayers D E and Lytle F W 1975 *Phys. Rev.* **B11** 4836
Tohji K, Udagawa Y, Kawasaki T and Masuda K 1983 *Rev. Sci. Instrum.* **54** 1482